



HAL
open science

Translation of rod-like template sequences into homochiral assemblies of stacked helical oligomers

Quan Gan, Xiang Wang, Brice Kauffmann, Frédéric Rosu, Yann Ferrand, Ivan
Huc

► **To cite this version:**

Quan Gan, Xiang Wang, Brice Kauffmann, Frédéric Rosu, Yann Ferrand, et al.. Translation of rod-like template sequences into homochiral assemblies of stacked helical oligomers. *Nature Nanotechnology*, 2017, 12 (5), pp.447-452. 10.1038/NNANO.2017.15 . hal-01520163

HAL Id: hal-01520163

<https://hal.science/hal-01520163>

Submitted on 9 May 2017

HAL is a multi-disciplinary open access archive for the deposit and dissemination of scientific research documents, whether they are published or not. The documents may come from teaching and research institutions in France or abroad, or from public or private research centers.

L'archive ouverte pluridisciplinaire **HAL**, est destinée au dépôt et à la diffusion de documents scientifiques de niveau recherche, publiés ou non, émanant des établissements d'enseignement et de recherche français ou étrangers, des laboratoires publics ou privés.

Translation of Rod-Like Template Sequences into Well-Defined Homochiral Assemblies of Stacked Helical Oligomers

Quan Gan,¹ Xiang Wang,¹ Brice Kauffmann,² Frédéric Rosu,² Yann Ferrand,¹ Ivan Huc^{1*}

¹ Université de Bordeaux, CNRS, IPB, CBMN – UMR 5248, Institut Européen de Chimie et Biologie, 2 rue Robert Escarpit, 33600 Pessac, France.

² Université de Bordeaux, CNRS, INSERM, IECB – UMS3033 – US01, Institut Européen de Chimie et Biologie, 2 rue Robert Escarpit, 33600 Pessac, France.

* Correspondence to: i.huc@iecb.u-bordeaux.fr

Translating a molecular sequence into a chemically different sequence has been powerfully exploited by nature, for example to produce proteins from mRNA templates. Yet, artificial systems inspired from this process are rare and far from optimized. Here we show that rod-like oligocarbamates may template the formation of well-defined sequences of stacked aromatic amide helices wound around them. Features of the rods, including the number and distance between carbamate functions and the presence of stereogenic centres, template the high fidelity formation of complementary stacks of helices each having a defined handedness, length and single or double helicity, through a self-assembly process allowing error correction. The outcome is unprecedentedly large abiotic folded architectures that may serve as scaffolds to organize appended functional features at positions in space defined with atomic precision across nanometric distances.

At the molecular level, translation refers to the production of a new entity according to a template that has a different chemical composition. Just like languages, chemical information may be translated from one molecule into another. The process of translation gives rise to structures and thus functions that might be difficult to create otherwise. It reaches exquisite levels of efficiency in biological systems as illustrated by protein expression from mRNA templates,^{1,2} or by the assembly of the tobacco mosaic virus capsid protein according to the length of its RNA.³ In synthetic systems, examples of molecules serving as a template to direct the synthesis of a structure of different chemical nature are numerous.⁴⁻⁶ But general and versatile schemes in which a non-natural sequence actually encodes the information necessary to produce a different sequence are very few and far from being optimized.⁷⁻¹⁰ In the following, we present the high-fidelity enzyme-free translation of long rod-like alkylcarbamate oligomers into well-defined sequences of stacked helical aromatic oligoamides each of which possibly differing by its length, its single or double helical state, and its right (*P*) or left (*M*) handedness (Fig. 1a). This process enables the production of very large (> 20 kDa) abiotic artificial folded architectures (*i.e.* foldamers¹¹) that may, for example, serve as scaffolds to organize appended functional features at positions in space defined with atomic precision across nanometric distances.

Helix-rod host-guest complexes termed foldaxanes have been shown to form upon winding aromatic oligomers around *para*-phenylenes,^{12,13} poly-alkylammoniums,¹⁴ or dicarbamates derived from α,ω -diaminoalkanes.^{15,16} In the latter case, arylamide foldamer hosts¹⁷ may be either single¹⁵ or double¹⁶ helical once wound around the rod (Fig. 1a, Fig. S1, Table S1). In this work, we use short oligomers **1**, **2** and **4** along with newly synthesized longer sequences **3**, **5**, **6** (Fig. 1b, Scheme S1) and rods **7-29** (Fig. 1b, Schemes S2-S7). Single station rods **7-14** served to assess the stability of host-guest complexes as a function of guest length. Association constants in CDCl₃

were systematically determined by ^1H NMR titrations (Table S2, Figs. S2 to S20). In addition, a Van't Hoff plot allowed us to calculate thermodynamic parameters for the formation of $(\mathbf{6})_2\supset\mathbf{15}$ as a representative example. The obtained values ($K_a = 590 \text{ mol.L}^{-1}$ at 293 K; $\Delta H = -41.3 \text{ kJ.mol}^{-1}$, $\Delta S = -89.0 \text{ J.K}^{-1}$, Fig. S21) reveal a strongly enthalpically driven process with a large entropic barrier. Complex formation involve hydrogen bonding between carbonyl groups of the guest and amide protons of 2,6-pyridinedicarboxamide units of the host, located at the two ends of the single helices, or at one end of each strand of the double helices. Consequently, a strict match is required between on one hand the distance between hydrogen bond donors on the helices (*i.e.* the number of helix turns) and on the other hand the length of the alkyl chains connecting hydrogen bond acceptors on the rods.¹⁵ In *single* helical complexes, shrinking the rod by a single CH_2 unit may result in a large or even complete loss of stability. In contrast, screw motions within the *double* helices allow them to adjust their length and to bind to rods differing by 3 to 4 CH_2 units with comparable affinities.¹⁶ This prior knowledge hinted at the possibility of loading numerous single and/or double helices, each having a defined length, on rods possessing the complementary binding stations arranged in a chosen sequence. The sequence would thus template the assembly of an organized multi-helical supramolecular polymer arrangement (Fig. 1a). Templatation would be facilitated by the facts that: (*i*) complex formation does not have to involve a threading mechanism which would require the stepwise introduction of the helices in the order of their arrangement on the rod. Instead, it may also occur *via* an unfolding of the helix and its refolding around the rod, allowing error correction in the process. Thermodynamic products may thus form regardless of the order in which components are assembled; (*ii*) both single and double helices may slide along the rods and find their best binding station without dissociating.^{15,16}

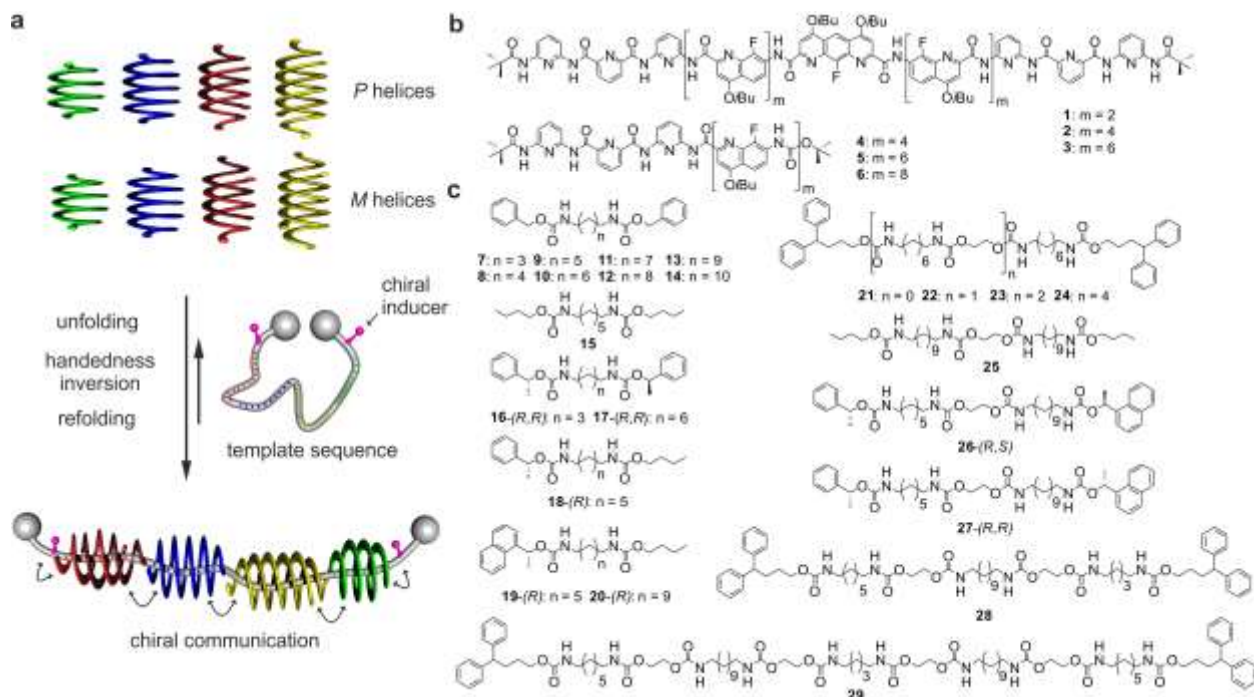


Figure 1. Principle of translation and molecules used. (a) Schematic representation of the controlled homochiral assembly of single and double stranded helices of various length onto a long dumbbell shaped template possessing complementary binding stations for each helix and terminal stereogenic centres. (b) Formulae of aromatic oligoamides forming single helical (**1-3**) and double helical (**4-6**) host-guest helix-rod complexes. In the absence of guest, all oligomers exist predominantly as double helices at thermodynamic equilibrium in 1 mM CDCl_3 solutions. (c) Formulae of oligocarbamate guest template sequences.

However, a major unsolved problem was the control of helix handedness. In the absence of transfer of chiral information from the rod into preferred handedness of the helix hosts, and in the absence of end-to-end helix-helix handedness communication between contiguous helices on the rod, the loading of numerous helices would only yield complex mixtures of diastereomeric helix arrangements all having a different spatial organization. Thus, we first aimed to control helix handedness using stereogenic centres on the rod. A series of rods having one helix binding station

and bearing one or two terminal chiral group were prepared (**16-20**, Scheme S2) and their host-guest complexes with single or double helical hosts of matching length were investigated (Figs. S22-S27 and S29-S30). As illustrated by the emergence of a major species in ^1H NMR spectra (Fig. 2a), the two chiral phenethyl groups on guest **16** efficiently induced the handedness of **2** (diastereomeric excess *d.e.* = 93%). A crystal structure of the **2**⊃**16** complex (Fig. 2e, Fig. S35, Table S3) allowed us to unambiguously assign *M* helicity as being favoured by (*R,R*) chirality on the rod. This resulted in a strong induced negative circular dichroism (CD) band at 342 nm whilst the (*S,S*) enantiomer induced a positive band (Fig. 2c). Diastereoselectivity was moderate when the rod possessed a single chiral group (**3**⊃**18**, see Fig. 2d), and also when the host was a double helix ((**5**)₂⊃**17**, see: Fig. 2f, Fig. S36, Table S4). Using a chiral terminal naphthylethyl group (**3**⊃**19** and (**6**)₂⊃**20**) gave rise to similar handedness induction.

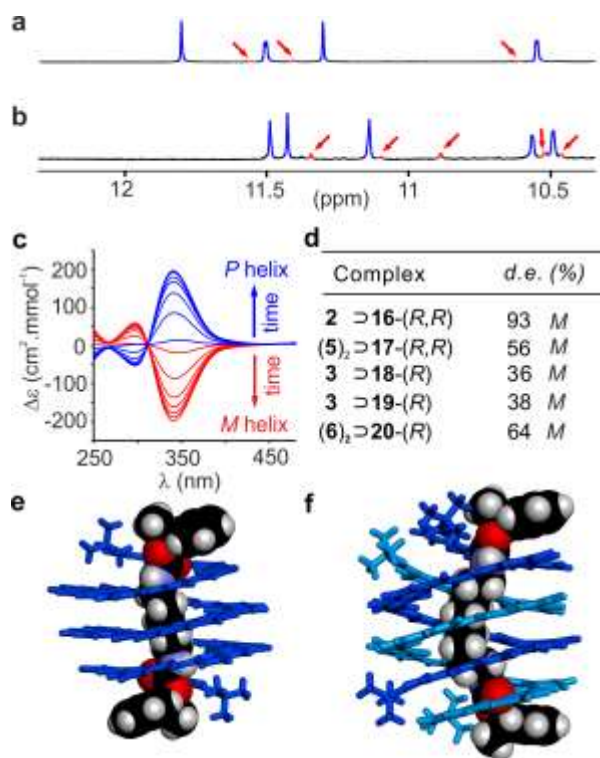


Figure 2. Foldaxane assembly, diastereoselectivity and helix handedness induction. Part of the 700 MHz ^1H NMR spectra in CDCl_3 at 298K of: (a) **2**⊃**16**-(*S,S*) with $[\mathbf{2}] = 1 \text{ mM}$ and $[\mathbf{16}-(\text{S,S})]$

= 2 mM; (b) $(\mathbf{6})_2 \supset \mathbf{20-(R)}$ with $[(\mathbf{6})_2] = 1$ mM and $[\mathbf{20-(R)}] = 2$ mM. Signals of major diastereomeric complexes are denoted in blue whereas minor complexes are denoted in red and pointed to with red arrows. (c) Circular dichroism (CD) spectra of $\mathbf{2}$ (20 μM , 313K) in CDCl_3 at different time intervals (5 min., 30 min., 60 min., 90 min., 120 min, 150 min. and 210 min.) after the addition of 3 equiv. of $\mathbf{16-(S,S)}$ (blue) or $\mathbf{16-(R,R)}$ (red). (d) *d.e.* values of helix-rod complexes defined as $d.e. = ([M \text{ helix}] - [P \text{ helix}]) / ([P \text{ helix}] + [M \text{ helix}]) \times 100$. The preferred helical sense is indicated next to *d.e.* values. (e) Tube (single helix) and CPK (rod) representation of the crystal structure of $P\text{-}\mathbf{2} \supset \mathbf{16-(S,S)}$. (f) Tube (double helix) and CPK (rod) representation of the crystal structure of $P\text{-}\mathbf{(5)}_2 \supset \mathbf{17-(S,S)}$. Isobutoxy side chains and included solvent molecules have been omitted for clarity.

Next, we assessed helix-helix end-to-end handedness communication when multiple helices were loaded on a multistation rod. Initial attempts using the double helix $(\mathbf{4})_2$ as a host showed that its affinity for guests of matching length was too low to achieve quantitative binding of several stations on a single rod at low mM concentration (Table S2). Longer oligomer $\mathbf{5}$ was thus prepared and shown to bind as a double helix to single station rod $\mathbf{21}$ with a K_a of 1700 M^{-1} in CDCl_3 at 298 K (Figs. 3b-d, 4B, S33, Table S5). Rods $\mathbf{22-24}$ possess two, three and five binding stations identical to that of $\mathbf{21}$ and may in principle bind to two, three or five $(\mathbf{5})_2$ duplexes, respectively. The stations are separated by an ethylene glycol spacer which plays a critical role in the design. Too short a spacer may cause steric hindrance between duplexes $(\mathbf{5})_2$ bound to contiguous stations resulting in negative binding cooperativity and eventually in unoccupied stations. Too long a spacer and the absence of contacts between adjacent duplexes may result in the absence of helix handedness communication, giving rise to complex mixtures of diastereomeric aggregates. Indeed, [5]foldaxane $(\mathbf{5})_4 \supset \mathbf{22}$ may exist as a pair of enantiomers *PP/MM* or as a *PM meso* species.

Similarly, [7]foldaxane (**5**)₆⊃**23** may exist as three distinct pairs of enantiomers and [11]foldaxane (**5**)₁₀⊃**24** as ten pairs of enantiomers (Fig. S31). Upon mixing (**5**)₂ with **22**, **23** or **24**, ¹H NMR initially showed complex patterns which simplified over time, eventually resulting in the emergence of a major species. Integration of the rod and helix signals established that the final aggregate stoichiometry corresponds to binding of helices to all stations on each rod (Figs. 4c-e, S32). In the case of **22** and **23**, the major species was unambiguously identified in the solid state by x-ray crystallography as being racemic homohelical (**5**)₄⊃**22** and (**5**)₆⊃**23**, in which all helices on a given rod have the same handedness (Figs. 3f-i, S38, S39, Tables S6, S7). Thus, contacts between helices having a "like" handedness are more favourable than contacts between helices having an "unlike" handedness, resulting in the translation of the sequence of stations on the rods into a well-defined arrangement of helical aromatic oligoamides. It was assumed that the same rule holds true for (**5**)₁₀⊃**24** of which a molecular model was built showing a 9 nm long structure (Fig. 3j, Movie S1). Single crystals of this very large complex (22 kDa) could also be obtained, but diffraction intensity was too weak to resolve the structure. The crystal structures of (**5**)₄⊃**22** and (**5**)₆⊃**23** revealed direct face-to-face π-π contacts between the helices. At each station, the alkyl moiety of the rod is slightly bent which makes its two ends protrude from the helix at an angle (see Fig. 3e). In contrast, the rods adopt a linear conformation at helix-helix junctions where a "like" handedness permits the same tilt angle of each helix with respect to the rod. This alternation of linear and bent segments of the rods gives rise to an undulated shape of the multi-helical aggregates.

The formation of homomeric multi-helical complexes was further studied in solution using double station rod **25** and double helix (**6**)₂ (Fig. S28). Upon saturation of the two-station rod, two duplexes are bound to form (**6**)₄⊃**25**. Aside for the major *PP/MM* species, minor signals assigned

to a *PM* diastereomer allowed to calculate a *d.e.* value above 90%. This value did not change significantly with temperature suggesting that more stable *PP/MM* diastereomers are favoured by enthalpy, with negligible involvement of entropy.

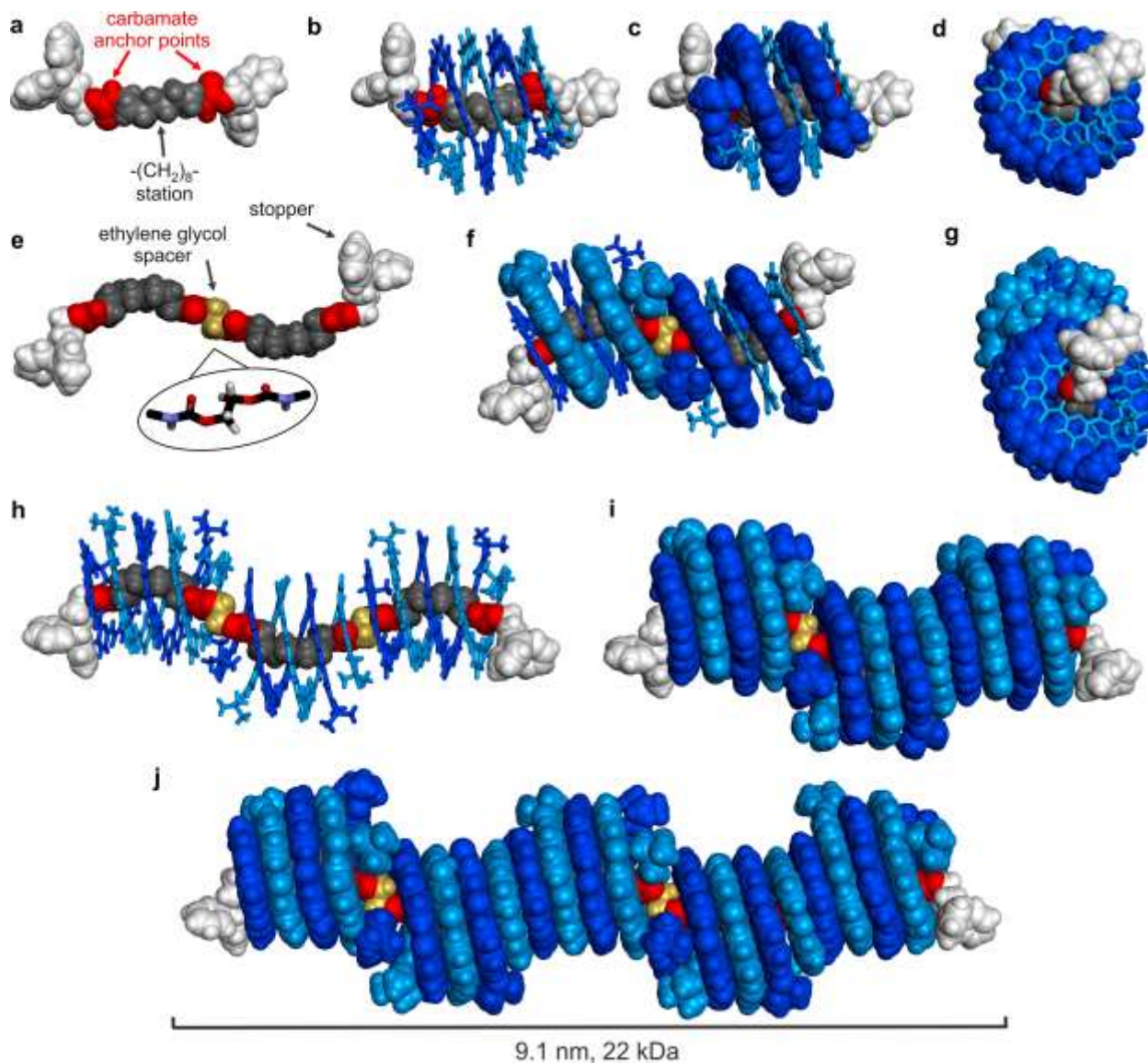


Figure 3. Structures in the solid state analyzed by single crystal x-ray crystallography of (a) dumbbell rod **21**; (b) $(5)_2D_{21}$ (side view) in CPK (Corey Pauling Koltun) and tube representations for the rod and the double helix, respectively; (c) $(5)_2D_{21}$ with one strand shown in CPK

representation; (d) $(\mathbf{5})_2\supset\mathbf{21}$ (top view); (e) rod $\mathbf{22}$; (f) $(\mathbf{5})_4\supset\mathbf{22}$ (side view) in CPK and tube/CPK representations for the rod and the double helix, respectively; (g) $(\mathbf{5})_4\supset\mathbf{22}$ (top view); (h) $(\mathbf{5})_6\supset\mathbf{23}$ (side view) in CPK and tube representations for the rod and the double helix, respectively. (i) $(\mathbf{5})_6\supset\mathbf{23}$ in full CPK representation. (j) Energy minimized molecular model using the Merck Molecular Force Field static (MMFFs) of the structure of $(\mathbf{5})_{10}\supset\mathbf{24}$. In (a-j) isobutoxy side chains and included solvent molecules were omitted for clarity. The rods $\mathbf{21}$, $\mathbf{22}$, $\mathbf{23}$ and $\mathbf{24}$ are shown as CPK representations whereas the helices $\mathbf{5}$ are shown as light blue/blue tube or CPK representations. Only the all *P* helical isomers are shown. The structures belong to centrosymmetrical space groups and thus also contain the all *M* isomers.

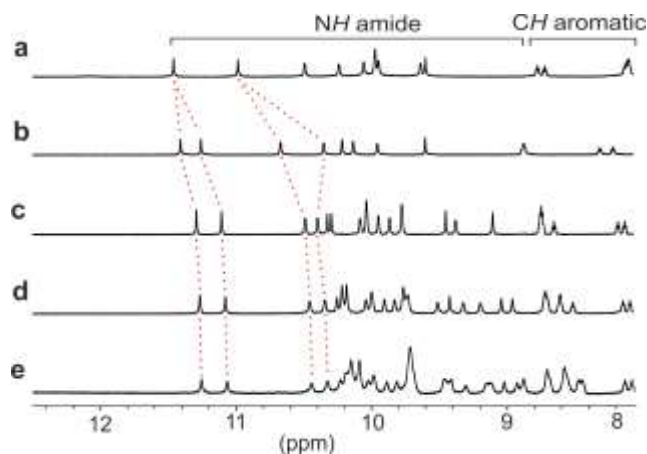


Figure 4. Solution evidence of unicity of the products. Part of the 700 MHz ¹H NMR in CDCl₃ (0.25 mM) showing the amide and some aromatic resonances of: (a) $(\mathbf{5})_2$; (b) $(\mathbf{5})_2\supset\mathbf{21}$; (c) $(\mathbf{5})_4\supset\mathbf{22}$; (d) $(\mathbf{5})_6\supset\mathbf{23}$ and (e) $(\mathbf{5})_{10}\supset\mathbf{24}$. Red dashes illustrate the shielding of terminal aromatic amide protons.

The production of well-defined homohelical arrays of aromatic oligoamides on sequences of alkyl carbamate rods represents a major advance with respect to other complexes between

polymers and helical or macrocyclic hosts in which no communication between the hosts takes place^{14,18-23} Efficient helix-helix end-to-end handedness communication in discrete aggregates amounts to exerting control over the piling up of helices into columns with preferred "like"²⁴⁻²⁶ or "unlike"²⁷ contacts as observed in the solid state.

Having established rod-helix and helix-helix chiral communication independently, we challenged ourselves to integrate all types of information that a rod may contain to be translated into an organized sequence of helices: chiral groups to control absolute helix handedness, several stations to bind to several helices, different stations to bind to different helices, *e.g.* a single and a double helix (Fig 5e). Rods **26** and **27** possess two distinct and long stations to ensure a high thermodynamic stability of their complexes with the matching helices, separated by an ethylene glycol spacer to induce helix-helix end-to-end handedness communication. A terminal phenethyl group is placed next to a station complementary to the single helix of **3**, and a terminal naphthylethyl group is placed next to a station complementary to the duplex (**6**)₂. Rods **26** and **27** differ from the relative stereochemistry of their two stereogenic centres which may favour the binding of two hosts having opposite handedness in the case of **26** or the same handedness in the case of **27**, thus acting either antagonistically or synergistically with respect to helix-helix handedness communication. Indeed, upon mixing **3** and (**6**)₂ with either **26**-(*R,S*) or **27**-(*R,R*), very different outcomes resulted. With **26**-(*R,S*), a complex NMR spectrum formed corresponding to a mixture of four possible *P(P)*₂, *M(M)*₂, *P(M)*₂ and *M(P)*₂ (**3**·(**6**)₂) \supset **26** complexes none of which had a strong prevalence (Fig. 5c). In contrast, with **27**-(*R,R*), a sharp ¹H NMR spectrum indicated the presence of a dominant species (Fig. 5d) whose structure was identified in the solid state as the favoured homohelical arrangement (Fig. 5e, 5f, S40, Table S8). The structure showed that the helix-helix end-to-end homohelical contact is similar for single helix-double helix communication

to that found for double helix-double helix communication. Thus, the stereogenic centres at each end of the rod as well as the helix-helix contact, although all remote from each other,²⁸ cooperatively contribute to the emergence of a complex multi-helical aggregate through the translation of information contained on a multistation guest.

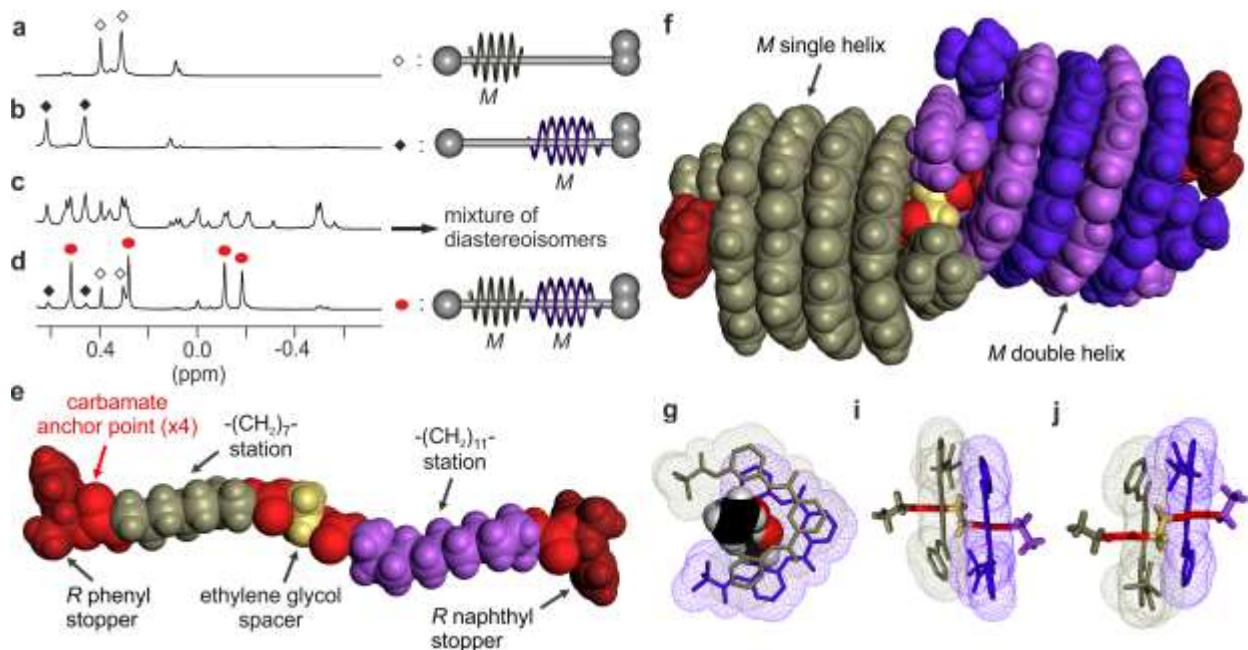


Figure 5. Formation of heteromeric stacks of oligomers on heteromeric rods. Part of the 400 MHz ^1H NMR spectra (resonances of the pivaloyl end groups of the helices) in CDCl_3 at 298K of: (a) $3 \supset 27-(R,R)$ (1 mM); (b) $(6)_2 \supset 27-(R,R)$ (1 mM); (c) 3 (1 mM) and $(6)_2$ (1 mM) in the presence of rod $26-(R,S)$ (1 equiv.); (d) 3 (1 mM) and $(6)_2$ (1 mM) in the presence of rod $27-(R,R)$ (1 equiv.). White diamonds denote $M-3 \supset 27-(R,R)$ whereas $M-(6)_2 \supset 27-(R,R)$ are marked with black diamonds. Red circles denote the homochiral complex $(M-3.M-(6)_2) \supset 27-(R,R)$. Side view of: (e) the crystal structure of rod $27-(R,R)$; (f) the crystal structure of $(M-3.M-(6)_2) \supset 27-(R,R)$. 3 is shown in grey and $(6)_2$ in purple and light purple. (g) Top view of the two pyridine trimers from 3 (grey tube) and $(6)_2$ (purple tube) which are shown to be in close contact and to hydrogen bond to the rod $27-(R,R)$ in CPK representation. (h) Side view from the same structure showing a kink (gold

tube) in **27**-(*R,R*). (i) Side view from the same structure with a 180° rotation along the rod axis. The volumes of the pyridine trimers of the single helix and one strand of the double helix are shown as grey taupe and purple isosurfaces, respectively, in quad mesh representation. Side chains (OiBu groups) and included solvent molecules have been removed for clarity.

The various helices **1-6** at our disposal selectively bind guests according to their length (Table S2) in such a way that three host-guest complexes may form with negligible cross-association: (**6**)₂⊃**13**, **3**⊃**9**, and **2**⊃**7** where **13**, **9** and **7** contain undecylene, heptylene and pentylene chains, respectively. For these three complexes, K_a values in CDCl₃ are above 10⁴ L.mol⁻¹ and cross association is inferior to 0.2 %. Complexes between **1** and shorter guests would not cross-associate but their use would be hampered by lower binding. Creating additional orthogonal helix-rod association would entail the preparation of longer helices and longer guests, or the use of other helix-rod binding modes.^{12-14,29} With these complexes in hands, we tested the possibility to increase information content during multi-foldaxane formation. Rods **28** and **29** were prepared which possess three and five helix-binding stations, respectively, of the three kinds mentioned above. The formation of the complexes was monitored by electrospray ion mobility mass spectrometry (ESI-IMMS) and confirmed the expected high fidelity loading of each helix according to the number of its corresponding binding station(s) on a given rod. Thus, the sequential loading of **3**, (**6**)₂, and **2** yielded each expected intermediate up to final complex **3.6₂.2**⊃**28** (Figure 6a-6c). Because of its large size (24kDa), the observation of **3.6₂.2.6₂.3**⊃**29** required to push instrumentation to its limits but was successful as well (Figure 6d). In addition, IMS gave access to the collision cross-sections (CCSs) of these objects in the gas phase. Calculated and measured values of foldaxanes from rods **21-24**, **28** and **29** are in excellent agreement (Figures 6e, 6f and

S33-34). The linear relation between CSSs and molecular mass is consistent with a rigid cylinder model³⁰ and suggests a long persistence length of the multihelix-rod complexes.

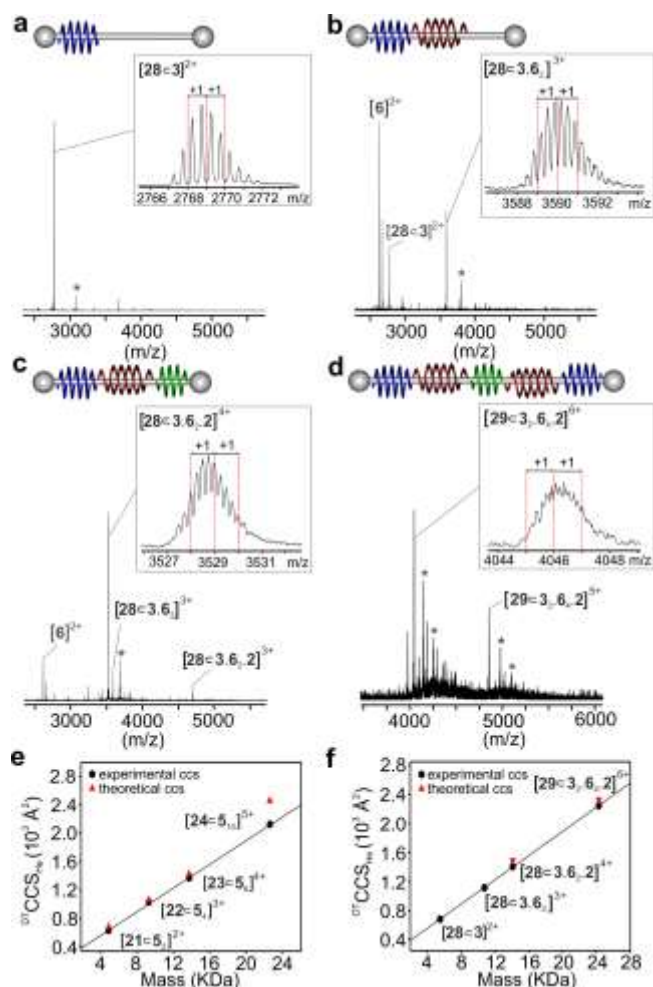


Figure 6. Detection of heteromeric stacks of oligomers on heteromeric rods using ion mobility mass spectrometry. Electrospray mass spectra (ESI-MS) of: (a) $3 \supset 28$; (b) $3.6_2 \supset 28$; (c) $3.6_2.2 \supset 28$; and (d) $3_2.6_4.2 \supset 29$, ([foldaxane] = 150 μM in CHCl_3). The peak annotation $[n]^{z+}$ indicates the number and nature of the foldamer n and the charge z of the detected complexes. Only the expected stoichiometries of the oligomers loaded on each rod are detected. Peaks marked with a star correspond to the expected masses +625 from an unidentified contaminant. (e,f) Comparison of collisional cross sections ($^{DT}CCS_{He}$, \AA^2) either experimental (\bullet) or calculated assuming a rigid

cylinder model (▲): (e) homomeric assemblies $5_2\supset 21$, $5_4\supset 22$, $5_6\supset 23$, $5_{10}\supset 24$; (f) heteromeric assemblies $3\supset 28$, $3.6_2\supset 28$, $3.6_2.2\supset 28$, $3_2.6_4.2\supset 29$.

In summary, we have established a robust and versatile scheme to produce well-defined homochiral arrangements of helical oligomers wound around multistation rod-like template guest sequences. Templates having up to ten urethane functions were used to form the largest abiotic folded architectures known to date. As other helix-rod recognition patterns are being identified,²⁹ the scheme may be further expanded and allow the organization in space of various functional groups attached to each helical component of a given assembly. Another extension would consist in optimizing the covalent capture³¹⁻³² of these non-covalent assemblies to convert the stack of helices into a single molecular polymeric chains. Developments along these lines will be reported in due course.

Methods. Methods and any associated references are available in the online version of the paper.

References

1. Moore, P. B., Steitz, T. A. The structural basis of large ribosomal subunit function. *Annu. Rev. Biochem.* **72**, 813–850 (2003).
2. Ogle, J. M., Ramakrishnan, V. Structural insights into translational fidelity. *Annu. Rev. Biochem.* **74**, 129–177 (2005).
3. Namba, K., Stubbs, G. Structure of tobacco mosaic virus at 3.6 Å resolution: implications for assembly. *Science* **231**, 1401–1406 (1986).
4. Petitjean, A., Nierengarten, H., van Dorsselaer, A., Lehn, J.-M. Self-organization of oligomeric helical stacks controlled by substrate binding in a tobacco mosaic virus like self-assembly process. *Angew. Chem. Int. Ed.* **43**, 3695–3699 (2004).
5. Suzuki, K., Sato, S., Fujita, M. Template synthesis of precisely monodisperse silica nanoparticles within self-assembled organometallic spheres. *Nat. Chem.* **2**, 25–29 (2010).
6. Kondratuk, D. V., Perdigão, L. M. A., Esmail, A. M. S., O’Shea, J. N., Beton, P. H., Anderson H. L. Supramolecular nesting of cyclic polymers. *Nat. Chem.* **7**, 317–322 (2015).

7. Lewandowski, B., De Bo, G., Ward, J. W., Pappmeyer, M., Kuschel, S., Aldegunde, M. J., Gramlich, P. M. E., Heckmann, D., Goldup, S. M., D'Souza, D. M., Fernandes, A. E., Leigh, D. A. Sequence-specific peptide synthesis by an artificial small-molecule machine. *Science* **339**, 189–193 (2013).
8. He, Y., Liu, D. R. Autonomous multistep organic synthesis in a single isothermal solution mediated by a DNA walker. *Nat. Nanotechnol.* **5**, 778–782 (2010).
9. McKee, M. L., Milnes, P. J., Bath, J., Stulz, E., Turberfield, A. J., O'Reilly, R. K. Multistep DNA-templated reactions for the synthesis of functional sequence controlled oligomers *Angew. Chem. Int. Ed.* **49**, 7948–7951 (2010).
10. Meng, W., Muscat, R. A., McKee, M. L., Milnes, P. J., El-Sagheer, A. H., Bath, J., Davis, B. G., Brown, T., O'Reilly, R. K., Turberfield, A. J. An autonomous molecular assembler for programmable chemical synthesis. *Nat. Chem.* **8**, 542–548 (2016).
11. Guichard, G., Huc, I. Synthetic foldamers. *Chem. Commun.* **47**, 5933–5941 (2011).
12. Tanatani, A., Mio, M. J., Moore, J. S. The size-selective synthesis of folded oligomers by dynamic templation. *J. Am. Chem. Soc.* **124**, 5934–5935 (2002)
13. Nishinaga, T., Tanatani, A., Oh, K., Moore, J. S. Chain length-dependent affinity of helical foldamers for a rodlike guest. *J. Am. Chem. Soc.* **123**, 1792–1793 (2001).
14. Petitjean, A., Cuccia, L. A., Schmutz, M., Lehn, J.-M. Naphthyridine-based helical foldamers and macrocycles: synthesis, cation binding, and supramolecular assemblies. *J. Org. Chem.* **73**, 2481–2495 (2008).
15. Gan, Q., Ferrand, Y., Bao, C., Kauffmann, B., Grélard, A., Jiang, H., Huc, I. Helix-rod host-guest complexes with shuttling rates much faster than disassembly. *Science* **331**, 1172–1175 (2011).
16. Ferrand, Y., Gan, Q., Kauffmann, B., Jiang, H., Huc, I. Template-induced screw motions within an aromatic amide foldamer double helix. *Angew. Chem. Int. Ed.* **50**, 7572–7575 (2011).
17. Zhang, D.-W., Zhao, X., Hou, J.-L., Li, Z.-T., Aromatic amide foldamers: structures, properties, and functions. *Chem. Rev.* **112**, 5271–5316 (2012)
18. Lee, C.-F., Leigh, D. A., Pritchard, R. G., Schultz, D., Teat, S. J., Timco, G. A., Winpenny, R. E. P. Hybrid organic–inorganic rotaxanes and molecular shuttles. *Nature* **458**, 314–318 (2009).
19. Talotta, C., Gaeta, C., Qi, Z., Schalley, C. A., Neri, P. Pseudorotaxanes with Self-Sorted Sequence and Stereochemical Orientation. *Angew. Chem. Int. Ed.* **52**, 7437–7441 (2013).
20. Lee, S., Chen, C.-H., Flood, A. H. A pentagonal cyanostar macrocycle with cyanostilbene CH donors binds anions and forms dialkylphosphate[3]rotaxanes. *Nat. Chem.* **5**, 704–710 (2013).
21. Belowich, M. E., Valente, C., Smaldone, R. A., Friedman, D. C., Thiel, J., Cronin, L., Stoddart, J. F. Positive cooperativity in the template-directed synthesis of monodisperse macromolecules, *J. Am. Chem. Soc.* **134**, 5243–5261 (2012).

22. Frampton, M. J., Anderson, H. L. Insulated molecular wires. *Angew. Chem. Int. Ed.* **46**, 1028–1064 (2007).
23. Harada, A., Li, J., Kamachi, M. The molecular necklace: a rotaxane containing many threaded α -cyclodextrins, *Nature* **356**, 325–327 (1992).
24. Sánchez-García, D., Kauffmann, B., Kawanami, T., Ihara, H., Takafuji, M., Delville, M.-H., Huc, I. Nanosized hybrid oligoamide foldamers: aromatic templates for the folding of multiple aliphatic units *J. Am. Chem. Soc.* **131**, 8642–8648 (2009).
25. Zhao, H., Ong, W. Q., Zhou, F., Fang, X., Chen, X., Li, S. F. Y., Su, H., Chob, N.-J., Zeng, H. Chiral crystallization of aromatic helical foldamers via complementarities in shape and end functionalities. *Chem. Sci.* **3**, 2042–2046 (2012).
26. Nakano, K., Oyama, H., Nishimura, Y., Nakasako, S., Nozaki, K. λ^5 -phospha[7]helicenes: synthesis, properties, and columnar aggregation with one-way chirality. *Angew. Chem. Int. Ed.* **51**, 695–699 (2012).
27. Haldar, D., Jiang, H., Léger, J.-M., Huc, I. Double versus single helical structures of oligopyridine-dicarboxamide strands. Part 2: the role of side-chains. *Tetrahedron* **63**, 6322–6330 (2007).
28. Clayden, J., Lund, A., Vallverdú, L., Helliwell, M. Ultra-remote stereocontrol by conformational communication of information along a carbon chain. *Nature* **431**, 966–971 (2004).
29. Gan, Q., Ferrand, Y., Chandramouli, N., Kauffmann, B., Aube, C., Dubreuil, D., Huc, I. Identification of a foldaxane kinetic byproduct during guest-induced single to double helix conversion. *J. Am. Chem. Soc.* **134**, 15656–15659 (2012).
30. Uetrecht, C., Rose, R. J., van Duijn, E., Lorenzen, K., Heck, A. J. R. Ion mobility mass spectrometry of proteins and protein assemblies. *Chem. Soc. Rev.* **39**, 1633–1655 (2010).
31. Clark, T. D., Ghadiri, M. R. Supramolecular design by covalent capture. Design of a peptide cylinder via hydrogen-bond-promoted intermolecular olefin metathesis. *J. Am. Chem. Soc.* **117**, 12364–12365 (1995).
32. Li, J., Carnall, J. M. A., Stuart, M. C. A., Otto, S. Hydrogel formation upon photoinduced covalent capture of macrocycle stacks from dynamic combinatorial libraries. *Angew. Chem. Int. Ed.* **50**, 8384–8386 (2011).

Acknowledgements. This work was supported by the Conseil Régional d'Aquitaine, the China Scholarship Council and by the European Research Council under the European Union's Seventh Framework Programme (Grant Agreement No. ERC-2012-AdG-320892). The authors thank

Christoph Mueller-Dieckmann (ESRF beamline ID29) for providing beamtime and help during data collection.

Author Contributions. Q.G. and X.W synthesized all new compounds and contributed equally to this work.. Q.G. and X.W. carried out solution studies. B.K. collected X-ray data and solved the crystal structures. F.R. carried out ion mobility mass spectrometry measurements. I.H. and Y.F. designed the study. I.H. and Y.F. wrote the manuscript. All authors discussed the results and commented on the manuscript.

Additional Information. Supplementary Information is linked to the online version of the paper at <http://www.nature.com/nature>. Materials and Methods; Schemes S1 to S7; Figs. S1 to S40; Tables S1 to S8; Movies S1 to S3. Crystallographic data for **2**→**16**, **(5)**₂→**17**, **(5)**₂→**21**, **(5)**₄→**22**, **(5)**₆→**23**, and **(3.(6)**₂)→**27** have been deposited with the Cambridge Crystallographic Data Centre under reference numbers CCDC-1482309, 1482270, 1482295, 1482290, 1482301, and 1482282 respectively. These data can be obtained free of charge from the Cambridge Crystallographic Data Centre (http://www.ccdc.cam.ac.uk/data_request/cif). Reprints and permissions information is available at <http://www.nature.com/reprints>. Correspondence and requests for materials should be addressed to I.H. (i.huc@iecb.u-bordeaux.fr).

Competing financial interests. The authors declare no competing financial interests.